NEOPLASMA accepted, ahead of print manuscript
Cite article as https://doi.org/10.4149/neo_2025_240918N387

Running title: Triptonide inhibits OSCC progression via TRIP13/c-Myc axis

Triptonide inhibits the progression of oral squamous cell carcinoma by suppressing the TRIP13/c-Myc axis

Hongbo Zhang[1], Zheng Wei[2], Shengwei Han[1], Sufeng Zhao[1,*]

[1]Department of Oral and Maxillofacial Surgery, Nanjing Stomatological Hospital, Affiliated Hospital of Medical School, Institute of Stomatology, Nanjing University, Nanjing, China; [2]Pediatric Dentistry, Nanjing Stomatological Hospital, Affiliated Hospital of Medical School, Institute of Stomatology, Nanjing University, Nanjing, China

*Correspondence: zsfnjkq@163.com

Received September 18, 2024 / Accepted January 28, 2025

Triptonide, an active ingredient of *Tripterygium wilfordii* Hook. F., has been found to have anticancer effects on various cancers; however, its effect on oral squamous cell carcinoma (OSCC) has not yet been studied. This study aims to reveal the effect and mechanism of triptonide on OSCC. The inhibitory effect of triptonide on OSCC progression was ascertained by CCK-8 assay, EdU incorporation assay, wound healing assay, Transwell assay, and xenograft tumor model, while western blotting, qRT-PCR, and immunohistochemistry revealed that triptonide could inhibit c-Myc expression in OSCC. RNA-Seq was conducted to explore the mechanism by which triptonide inhibited the progression of OSCC, and thyroid hormone receptor interactor 13 (TRIP13) was identified as a key differentially expressed gene. TRIP13-knockdown OSCC cells constructed with siRNA showed weaker progression ability in CCK-8 assay, EdU incorporation assay, wound healing assay, and Transwell assay. Finally, TRIP13-overexpressing OSCC cells constructed through plasmid were used in rescue experiments, which demonstrated that TRIP13 was located upstream of c-Myc and the overexpression of TRIP13 could partially restore the decreased c-Myc expression caused by triptonide treatment. Collectively, this study demonstrated that triptonide might reduce the expression of c-Myc by suppressing TRIP13 expression, thereby inhibiting the progression of OSCC. These findings have revealed a partial mechanism by which triptonide acts on OSCC and suggested its potential application value in OSCC treatment.

Key words: triptonide; oral squamous cell carcinoma; c-Myc; thyroid hormone receptor interactor 13; progression

Oral squamous cell carcinoma (OSCC) is the most prevalent type of malignant tumor in the oral cavity, accounting for 90% of all cases of oral cancer on a global scale [1]. In recent years, the number of new cases and mortality from OSCC has exceeded 370,000 and 170,000, respectively, on

an annual basis [2]. The consequences of OSCC for patients include disfigurement and functional impairment, including swallowing, speech, and taste, which have a substantial impact on the quality of life of patients [3]. Current treatment options for OSCC patients include surgery, radiotherapy, chemotherapy, biologic therapy, and molecular targeted therapy [4]. Despite considerable progress in recent decades, the 5-year survival rate for OSCC patients remains at approximately 60%, largely due to tumor metastasis and subsequent recurrence [1, 5]. Consequently, there is a significant need to identify and develop drugs that can effectively inhibit the progression of OSCC and elucidate their underlying mechanisms of action.

Triptonide, a diterpenoid, is one of the main active ingredients of a Chinese herb called *Tripterygium wilfordii* Hook. f. (TWHF), and has been shown to have structural similarity to triptolide, another active ingredient of TWHF, which has been demonstrated to have anticancer effects in a number of tumors [6]. Triptonide possess pharmacological activities, including anti-tumor and anti-inflammatory properties, while exhibiting significantly reduced toxicity in comparison to triptolide [7]. A growing body of research has demonstrated that triptonide exerts substantial antitumor effects in various tumor models through multiple mechanisms [8-12]. However, the anti-tumor role of triptonide in OSCC remains to be elucidated.

The members of the oncoprotein MYC family are pleiotropic transcription factors that modulate global gene expression and regulate critical cellular processes, including proliferation, differentiation, the cell cycle, metabolism and apoptosis. Among them, c-Myc is closely related to the progression of tumors, with c-Myc being dysregulated in 70% of human cancers and generally linked to a poor prognosis [13-15]. There is a substantial body of evidence supporting the notion that aberrant c-Myc expression is a critical driver of tumor initiation and maintenance, and is associated with all the "hallmark" features of cancer [16]. Studies have shown that c-Myc expression increases in OSCC and plays a pivotal role in cell survival/proliferation and cancer development [17, 18]. Our previous study found that c-Myc expression was closely correlated with the prognosis and immune cell infiltration of OSCC [19]. Therefore, the targeting of c-Myc with small molecule drugs may represent an effective approach to the treatment of OSCC. Studies have shown that triptonide can promote the apoptosis of acute myeloid leukemia cells by inhibiting the expression of c-Myc [20, 21]. Our previous study has also confirmed that triptonide can inhibit the expression of c-Myc in OSCC cells [19]. However, the mechanism by which triptonide inhibits c-

Myc expression remains unclear.

Thyroid hormone receptor interactor 13 (TRIP13) is a member of the highly conserved AAA+ protein family (ATPases associated with diverse cellular activities), and is classically considered a regulator of chromosomal events, including meiotic DNA break formation and recombination, chromosome synapsis and mitotic checkpoint regulation, which accounts for the chromosomal instability in most human cancers [22]. A substantial body of research has demonstrated that TRIP13 is highly expressed in various human cancers, including cervical cancer, thyroid cancer, colorectal cancer, and bladder cancer, and that it promotes the occurrence and development of cancers through multiple mechanisms [23-26]. Consequently, TRIP13 may be a therapeutic target for human cancers. Several studies have demonstrated that TRIP13 overexpression enhances drug resistance and radiation resistance in head and neck cancer [27, 28]. However, the role and mechanism of TRIP13 in OSCC progression remains poorly understood.

In this study, we investigated the impact of triptonide on the proliferation, migration, invasion, and c-Myc expression of OSCC cells. Utilizing RNA-Seq, we identified the differentially expressed gene TRIP13 in OSCC following triptonide treatment and examined its function in OSCC progression. The study demonstrated that triptonide could potentially inhibit c-Myc expression in OSCC by modulating TRIP13, thereby enhancing the comprehension of the mechanisms through which triptonide exerts its anticancer effects. The study also proposed the TRIP13/c-Myc axis for the first time and confirmed the association between these two oncogenes, which provides a valuable avenue for cancer treatment by indirectly targeting c-Myc.

Materials and methods

Materials and cell culture conditions. Triptonide (purity > 98%) was purchased from Sigma (MO, USA) and dissolved in dimethyl sulfoxide (DMSO) as a 5 mM stock solution. This solution was then freshly diluted in culture media at different concentrations. The human tongue squamous cell carcinoma cell line CAL27 was obtained from the Type Culture Collection of the Chinese Academy of Sciences (Shanghai, China). The CAL27 cells were cultivated in Dulbecco's modified Eagle's medium (DMEM; Gibco, NY, USA) supplemented with 10% fetal bovine serum (FBS; Biological Industries, Israel), 100 $U.ml^{-1}$ penicillin and 100 $mg.ml^{-1}$ streptomycin (KeyGen, Jiangsu, China) in a humidified atmosphere containing 5% CO_2 and 20% O_2 at 37 °C.

Cell Counting Kit-8 (CCK-8). The CCK-8 assay was performed using a CCK-8 kit (DOJINDO Laboratories, Kumamoto, Japan) according to the manufacturer's instructions. Briefly, cells were seeded at a density of 5×10^4 cells/well in 96-well plates in 100 µl complete culture medium and cultured for a specified time. CCK-8 (5 µl) was then added to each well and after 2 h, the optical density (OD) values were read at 450 nm using a microplate reader (SpectraMax M3; Molecular Device, CA, USA).

5-Ethynyl-2′-deoxyuridine (EdU) incorporation assay. The EdU incorporation assay was performed separately using a keyFluor594 Click-iT EdU Flow Cytometry Kit and a kFluor488 Click-iT EdU Flow Cytometry Kit (KeyGen, Jiangsu, China) according to the manufacturer's instructions. Treated cells were incubated with EdU-containing medium at a concentration of 50 µM for 2 h, after which they were collected, fixed and stained. Then, cell proliferation was detected using a flow cytometer (CytoFLEX; BECKMAN COULTER, CA, USA) and analyzed using FlowJo 10 software (Tree Star, OR, USA).

Wound healing assay. Cells in the logarithmic growth phase were seeded in six-well plates and grown to confluence. Then, cells were delineated with 200 µl pipette tips to create scratch zones in the cell monolayer and washed twice with PBS. Changes in cell scratch spacing were recorded by photographs taken at 0 and 24 h under a microscope (IX51; OLYMPUS, Tokyo, Japan) and quantified to assess cell migration using ImageJ software (National Institutes of Health, MD, USA).

Transwell assay. The cell invasion assay was conducted using a transwell system equipped with 6.5 mm insert chambers (Corning, NY, USA). Cells were seeded at a density of 1×10^5 cells/well with 100 µl serum-free culture medium on the top chamber of the transwell coated with Matrigel (BD Biosciences, NJ, USA). Complete culture medium (20% FBS, 500 µl/well) was added to the bottom chamber. After incubation for 24 h at 37 °C, the cells were fixed with 4% paraformaldehyde and stained with 0.1% crystal violet (Sigma, MO, USA). Cells remaining on the upper surface were completely removed and the invaded cells were photographed using an inverted microscope (IX51; OLYMPUS, Tokyo, Japan). Three random fields of view were captured for each well to facilitate cell counting.

Xenograft tumor model. The NOD-SCID female mice (n=10, 4-6 weeks old) were purchased from Shanghai Lingchang Biotechnology Co., Ltd (Shanghai, China) and maintained in a specific pathogen-free environment. CAL27 cells were injected subcutaneously into the right axillary region

of each mouse (2×10^7/ml, 0.1 ml/site). When the tumor volume reached approximately 100 mm^3, 10 mice were randomly divided into a control group and a triptonide treatment group. The mice in the treatment group were injected intraperitoneally with triptonide at a dose of 5 mg/kg once a day, while the control group was injected with physiological saline. The animal weights and tumor volumes were measured every 3 days (tumor volume=0.5 × long axis × short $axis^2$). After 21 days, the mice were euthanized, and the tumors were dissected, weighed, and used for subsequent immunohistochemistry (IHC). The animal studies were performed in accordance with the Guide for the Care and Use of Laboratory Animals, and all animal experiments and experimental protocols were approved by the Nanjing Stomatological Hospital Ethics Committee (approval number: NJSH-2021NL-58).

Western blotting (WB). WB was conducted in accordance with the established protocol [29]. The primary antibodies used were as follows: rabbit anti-GAPDH (1:5000, KGC6102-1, KeyGen, Jiangsu, China), mouse anti-c-Myc (1:10000, 67447-1-Ig, Proteintech, Hubei, China) and rabbit anti-TRIP13 (1:1000, AF0570, Affinity Biosciences, Jiangsu, China). The secondary antibodies used were as follows: goat anti-rabbit IgG-HRP (KGC6202-0.1, KeyGen, Jiangsu, China) and goat anti-mouse IgG-HRP (KGC6203-0.1, KeyGen, Jiangsu, China).

RNA extraction and qRT-PCR. Total cellular RNA was extracted using TRIZOL reagent (Invitrogen, CA, USA) according to a standard protocol. The PrimeScript™ RT reagent kit with gDNA Eraser (Takara, Kyoto, Japan) was utilized for RNA reverse transcription. Quantitative real-time PCR (qRT-PCR) was performed on an Applied Biosystems ViiA™7 instrument using a ChamQ Universal SYBR qPCR Master Mix (Vazyme, Jiangsu, China) according to the manufacturer's protocol. Gene expression was normalized to GAPDH expression. The quantification of mRNA was performed using the $2-\Delta\Delta Ct$ method. Three biological replicates were set up for each sample assay to reduce experimental error. The primer sequences used were as follows: c-Myc (Forward: 5′-GTAGTGGAAAACCAGCAGCC-3′, Reverse: 5′-CCTCCTCGTCGCAGTAGAAA-3′); GAPDH (Forward: 5′-CAAATTCCATGGCACCGTCA-3′, Reverse: 5′-AGCATCGCCCCACTTGATTT-3′); TRIP13 (Forward: 5′-TCATATACCCTCGCCAGCAG-3′, Reverse: 5′-CTGGACATACAGCGCATGAG-3′).

IHC staining. Paraffin-embedded tumor tissue sections (5 μm) were dewaxed in xylene, hydrated in gradient ethanol, and boiled in 0.01 M citrate buffer (pH 6.0) for 10 min for antigen recovery.

The sections were then incubated with mouse anti-c-Myc (1:100, 67447-1-Ig, Proteintech, Hubei, China) overnight at 4 °C. Subsequently, a horseradish peroxidase-linked secondary antibody was added for 10 min at room temperature, and diaminobenzidine (DAB) substrate was added for observation. Finally, the films were restained with hematoxylin and sealed with an aqueous sealer. The results were imaged under a fluorescence microscope (BX63; OLYMPUS, Tokyo, Japan).

RNA-seq. CAL27 cells were divided into 3 groups: NC group, 50 nM group, and 100 nM group, with three samples in each group. The cells in the NC group were incubated in the complete medium for 48 h, while the cells in the 50/100 nM group were treated with triptonide at the dose of 50/100 nM in the complete medium for 48 h. The cells were collected and lysed using the TRIzol solution. RNA- seq was performed by KeyGen Biotech Co. Ltd. (Jiangsu, China) using an Illumina Hiseq Sequencing platform. String Tie was used to evaluate the expression levels of mRNAs by calculating fragments per kilobase million (FPKM). Raw data from RNA- seq of all samples were averaged, and then the respective data from the samples were transformed as the provider divided by the average (mean). Differentially expressed genes were selected with $|\log2FoldChange| > 1$ and p-value < 0.05. Gene Ontology (GO) and Kyoto Encyclopedia of Genes and Genomes (KEGG) pathway enrichment analysis were used to detect gene pathways with significant changes after triptonide treatment.

Cell transfection. Synthetic TRIP13 siRNAs and negative control siRNA were purchased from KeyGen (Jiangsu, China) and for the construction of the TRIP13 knockdown CAL27 cell lines and their control. The sequences of the siRNAs were as follows: TRIP13 siRNA 1 (target sequence: 5′-GUGAAAAUCUGGAGGAAGATT-3′, antisense: 5′-UCUUCCUCCAGAUUUUCACTT-3′); TRIP13 siRNA 2 (target sequence: 5′-ACAAGAACGUCAACAGCAATT-3′, antisense: 5′-UUGCUGUUGACGUUCUUGUTT-3′); TRIP13 siRNA 3 (target sequence: 5′-CCUGAGUGUUAGAAAGCUATT-3′, antisense: 5′-UAGCUUUCUAACACUCAGGTT-3′). The plasmids for TRIP13 overexpression and negative control were constructed using the pcDNA3.1 vector (KeyGen, Jiangsu, China). When the CAL27 cells reached 70% confluence, the siRNAs and plasmids were transfected using the KeygenMAX 3000 transfection kit (KeyGen, Jiangsu, China) according to the manufacturer's protocol. After transfection, the mRNA and protein levels of TRIP13 were assessed at 48 h.

Statistical analysis. GraphPad Prism 9.0 (GraphPad Software Inc., CA, USA) was used to analyze

and plot the experimental results, including Student's t-test for comparisons between two groups and one-way ANOVA for comparisons between multiple groups. For all statistical analysis, $p < 0.05$ was considered statistically significant.

Results

Triptonide inhibited the progression of OSCC. Firstly, we evaluated the appropriate concentration and duration for triptonide to exert inhibitory effect on CAL27 cells by CCK-8 assay and found that there was no significant difference among the effects of different concentrations from 0 to 100 nM of triptonide on the viability of CAL27 cells for 24 h. However, after 48 and 72 h of treatment, the viability of CAL27 cells significantly decreased with increasing triptonide concentration (Figure 1A). The IC50 of CAL27 cells treated with triptonide for 48 and 72 h were 88.54 nM and 81.58 nM, respectively. We then detected the changes in the proliferation ability of CAL27 cells after treatment with different concentrations of triptonide for 48h through EdU incorporation assay and found that treated cells showed lower EdU fluorescence positive rates compared to untreated cells, which revealed that triptonide treatment markedly inhibited the proliferation ability of CAL27 cells (Figure 1B). Subsequently, the wound healing assay and transwell assay (Figures 1C, 1D) were employed to observe the effects of triptonide on cell migration and invasion. The results demonstrated a decrease in cell migration distance and the number of invaded cells with an increase in triptonide concentration, suggesting that triptonide treatment also inhibited the migration and invasion ability of CAL27 cells. Furthermore, we established a xenograft model of OSCC by subcutaneously injecting CAL27 cells into the right axillary region of each mouse. The weights of mice and the volumes of tumors were recorded during the triptonide vs placebo treatment. The results demonstrated that tumor volumes increased significantly more slowly in the triptonide treatment group than in the control group, while there was no significant difference in the weight gain of mice between the two groups (Figure 1E). Following a 21-day treatment period, the tumors were dissected and weighed, and we found that the tumor weights in the triptonide treatment group were significantly lower than those in the control group (Figure 1F). These findings provide substantial evidence for the inhibitory effect of triptonide on the progression of OSCC.

Triptonide inhibited the c-Myc expression in OSCC. Subsequently, we detected the alterations of

c-Myc mRNA and protein expression in CAL27 cells after triptonide (50 nM) treatment by qRT-PCR and WB, and found a substantial decrease in the expression of c-Myc mRNA and protein in CAL27 cells after triptonide treatment (Figures 2A, 2B). IHC c-Myc staining was performed on the dissected tumors mentioned above, and the results showed that the positive area and staining intensity of c-Myc in OSCC tissues were visibly reduced after triptonide treatment compared with those in the control group (Figure 2C). Combined with our past study [19], we demonstrated here that triptonide could inhibit the expression of c-Myc in OSCC.

Triptonide drives transcriptome changes in OSCC cells *in vitro*. To explore the mechanism by which triptonide inhibits OSCC progression and c-Myc expression, we performed RNA-seq to detect the global gene expression profiles on triptonide (50 nM)-treated, triptonide (100 nM)-treated and control CAL27 cells, with 3 replicates in each group. Differentially expressed genes were selected with $|\log2FoldChange| > 1$ and p-value < 0.05. Subsequent cluster analysis on differential expression genes in the three groups revealed that triptonide (50 nM)- treated samples, triptonide (100 nM)- treated samples and control samples were grouped into three clusters, suggesting good repeatability of the experiments (Figure 3A). 1435 genes were downregulated and 2474 genes were upregulated in triptonide (50 nM)-treated cells compared to the control cells (Figure 3B), while 1084 genes were downregulated and 2191 genes were upregulated in triptonide (100 nM)-treated cells compared to the control cells (Figure 3C).

Through GO enrichment analysis, we found that DNA replication and DNA-dependent DNA replication pathways were the most significantly enriched pathways with the highest rich factors after triptonide (50 nM) treatment (Figures 3D, 3E), and triptonide (100 nM) treatment showed similar results (Supplementary Figures S1A, S1B). GO enrichment analysis of downregulated differentially expressed genes after triptonide (50 nM) treatment also showed DNA replication and DNA-dependent DNA replication pathways were the most significantly enriched pathways with the highest rich factors (Figure 3F), the same as triptonide (100 nM) treatment (Supplementary Figure S1C), while GO enrichment analysis of upregulated differentially expressed genes did not (Supplementary Figures S1D, S1E). Similarly, KEGG pathway enrichment analysis revealed that the differentially expressed genes were enriched in the DNA replication pathway with the highest rich factors after the treatment with both 50 nM (Figure 3G) and 100 nM triptonide (Supplementary Figure S2A). KEGG pathway enrichment analysis of downregulated differentially expressed genes

after the treatment of 50 nM and 100 nM triptonide displayed the same results (Figure 3H, Supplementary Figure S2B), while KEGG pathway enrichment analysis of upregulated differentially expressed genes did not (Supplementary Figures S2C, S2D). These results suggested that triptonide might inhibit OSCC progression and c-Myc expression mainly by affecting DNA replication, and the key gene was located in the downregulated differentially expressed genes.

In order to narrow down the scope, we further selected downregulated differentially expressed genes with fold change < 0.25 and p-value < 0.001 after triptonide treatment and screened 225 genes in the 50 nM group and 124 genes in the 100 nM group. We found 96 common genes in the two groups of genes (Figure 4A), suggesting a high consistency in differentially expressed genes between the two groups. By consulting the relevant literature, we identified TRIP13 as the key differential gene for further research. Utilizing Gene Expression Profiling Interactive Analysis (GEPIA) [30], we observed that TRIP13 was highly expressed in the vast majority of tumor types (Figure 4B), including HNSCC (Figure 4C), and was positively associated with the expression of MYC (Figure 4D). To verify the result of RNA-seq, we detected the changes of TRIP13 expression in CAL27 cells after triptonide (50 nM) treatment by WB and qRT-PCR, and found that the mRNA and protein levels of TRIP13 significantly decreased after triptonide treatment (Figures 4E, 4F).

Knockdown of TRIP13 inhibited the progression of OSCC. To investigate the role of TRIP13 in OSCC progression, we constructed three TRIP13 knockdown CAL27 cell lines by siRNA transfection and verified their TRIP13 knockdown efficiency by qRT-PCR and WB. The results showed that TRIP13 mRNA and protein expression were knocked down by more than 50% in all three cell lines compared to the control groups (Figures 5A, 5B). Following this, the most efficient of the three siRNAs designed to target TRIP13 was selected for further study. The CCK-8 assay revealed that the viability of CAL27 cells was significantly reduced by the downregulation of TRIP13 in comparison to the control groups (Figure 5C). Similarly, the EdU incorporation assay demonstrated that TRIP13 knockdown significantly inhibited the proliferation ability of CAL27 cells (Figure 5D). Finally, as revealed by the wound healing assay and transwell assay (Figures 5E, 5F), the migration distances of cells and the numbers of invaded cells of the TRIP13 knockdown group were fewer than those of the control groups, indicating that TRIP13 knockdown also decreased the migration and invasion ability of CAL27 cells. These results demonstrated that TRIP13 played a cancer-promoting role in OSCC, and that the knockdown of TRIP13 could inhibit

the progression of OSCC.

TRIP13 overexpression partially restored the decreased c-Myc expression after triptonide treatment in OSCC cells. Finally, we constructed a TRIP13 overexpressing CAL27 cell line and a negative control cell line through plasmid transfection, and validated their overexpression efficiency by qRT-PCR (Figure 6A) and WB (Figure 6B), with satisfactory results. We used these cell lines for the final rescue experiments and grouping as shown in the figure. The rescue experiments revealed that the knockdown of TRIP13 alone led to a reduction in c-Myc expression, while the overexpression of TRIP13 resulted in a partial restoration of c-Myc expression that had been diminished by triptonide treatment in CAL27 cells (Figures 6C, 6D). This finding suggested that triptonide might reduce c-Myc expression in OSCC cells by inhibiting TRIP13 expression.

Discussion

In recent years, triptonide has attracted significant attention for its pharmacological activities, mainly including anti-tumor, anti-inflammatory, anti-androgenic reproductive function, etc., of which the anti-tumor effect is particularly prominent [7]. Triptonide has emerged as a promising potential anticancer agent, demonstrating the capacity to elicit anticancer effects in various types of cancers through different biological mechanisms. Wang et al. found that triptonide can inhibit the malignant behaviors of lung cancer cells by down-regulating the expression of the key oncogenic factor SOX2 through an epigenetic regulation mechanism [8]. Xiang et al. found that triptonide can inhibit the migratory and invasive abilities of gastric cancer cells by promoting the ubiquitination-mediated degradation of Notch1 protein [9]. A study showed that triptonide can suppress triple-negative breast cancer (TNBC) cell tumorigenesis, vasculogenic mimicry and invasion via degradation of Twist1 and Notch1 oncoproteins, downregulation of metastatic and angiogenic gene expression, and reduction of NF-κB signaling pathway [10]. Furthermore, triptonide has been shown to induce excess ROS production and oxidative stress and subsequently lead to endoplasmic reticulum stress (ERS)-mediated apoptosis by inducing p38 and the ERK–MAPK signaling pathway in osteosarcoma [11]. In addition, triptonide can exert potent anti-lymphoma effect with low toxicity by inhibiting proto-oncogene Lyn transcription and suppressing the downstream ERK and ATK signaling pathways [12]. However, the potential of triptonide in the treatment of OSCC has not been previously investigated, thus creating a knowledge gap that this study sought to

address. Our research showed that, as in other cancers, triptonide could significantly inhibit the proliferation, migration, and invasion of OSCC cells *in vitro*. Meanwhile, the xenograft tumor assay confirmed that triptonide could inhibit the progression of OSCC *in vivo*. Furthermore, the RNA-seq results suggested that triptonide exerted anticancer effects in OSCC mainly by affecting DNA replication, which revealed the potential value of triptonide in the treatment of OSCC and laid the groundwork for further research. Triptolide and triptonide are the main bioactive diterpenes isolated from TWHF. The chemical structures of these two compounds differ in terms of substituent groups at the C-14 position, with triptolide having a C-14-hydroxyl group and triptonide possessing a C-14-carbonyl group [31]. Studies have shown that compared to more extensively studied triptolide, triptonide induced significantly less hepatotoxicity and nephrotoxicity [32, 33]. In the xenograft tumor assay, no significant difference in body weight of mice was observed between the triptonide treatment group and the control group over 21 days, indicating that the short-term acute toxicity of triptonide is not notable. A study exploiting the role of triptonide in inhibiting mature sperm cells during spermatogenesis to develop a male contraceptive agent showed that neither short-term nor long-term triptonide treatment caused any discernable systematic toxic side effects in monkeys [34]. Nevertheless, the long-term and chronic toxicity of triptonide in humans requires further evaluation. With the further elucidation of the molecular mechanisms underlying the multiple pharmacological effects of triptonide, and the development of methods to enhance its efficacy and reduce toxicity, it will have a broad prospect for development and application in the field of anticancer.

c-Myc is a pivotal regulator of numerous biological programs, primarily functioning as a transcription factor that modulates the expression of thousands of genes. It is estimated that approximately 15% of genes in the genome are subject to c-Myc regulation [35]. c-Myc aberrations or upregulation of c-Myc-related pathways by alternate mechanisms occur in the vast majority of cancers. Details on how c-Myc biologically modulates cancer cell-intrinsic programs of cellular proliferation, differentiation, survival and death have been described elsewhere [36-38]. It is worth mentioning that c-Myc activates cellular survival programs through specific effects on DNA replication and can directly activate the DNA replication machinery [39], which is consistent with the above RNA-seq results, suggesting a prominent role for c-Myc in the anticancer effects exerted by triptonide. Research has shown that the increased expression of c-Myc in OSCC is closely associated with the poor prognosis and plays a key role in cell survival/proliferation and cancer

development [17-19]. A large number of studies have demonstrated that suppression of c-Myc signaling can result in sustained tumor regression, suggesting that targeting c-Myc could be an effective approach against a multitude of human cancers, including OSCC. The development of novel agents to target c-Myc should be a high priority and a promising approach for applying targeted therapeutic strategies for cancer therapy. Numerous therapeutic agents that directly target c-Myc are currently under development, but to date their clinical efficacy remains to be demonstrated. Several conceptual and practical difficulties, including its nuclear localization, the lack of a defined ligand binding site, and the physiological function essential to the maintenance of normal tissues have made c-Myc difficult to target [40, 41]. Therefore, exploring strategies for indirectly targeting c-Myc has emerged as a prominent research focus, encompassing approaches such as decreasing c-Myc biosynthesis or altering its stability, reducing c-Myc mRNA stability, targeting upstream regulators to inhibit c-Myc transcription, targeting c-Myc synthetic metabolic vulnerabilities, etc. [15]. In this study, we found that triptonide could effectively inhibit the expression of c-Myc in OSCC cells and tissues, which is consistent with the results observed in other types of cancer [20, 21, 42], suggesting the potential of triptonide as a small-molecule drug targeting c-Myc to exert anticancer effects. However, the mechanism by which triptonide inhibits c-Myc expression is not yet clear. Here, we have conducted a preliminary exploration of this question.

As c-Myc is such an important transcription factor in cells, it is subject to exquisite regulation, with many upstream proteins of c-Myc exhibiting elevated expression in tumors. Utilizing RNA-seq, we identified TRIP13, which is also closely associated with DNA replication, as a key differentially expressed gene following triptonide treatment in CAL27 cells. We hypothesized that TRIP13 plays a role in the triptonide-induced downregulation of c-Myc, and confirmed that the expression of TRIP13 in OSCC cells significantly decreased after triptonide treatment, and TRIP13 knockdown alone suppressed the proliferation, migration, and invasion of OSCC cells. These findings suggested that triptonide could suppress the progression of OSCC by regulating TRIP13. Research has demonstrated that TRIP13 can promote lung cancer cell growth and metastasis through AKT/mTORC1/c-Myc signaling [43]. Zhang et al. found that TRIP13 can promote the proliferation, migration and invasion of glioblastoma cells through the FBXW7/c-MYC axis [44]. Liu et al. discovered that in breast cancer cells, TRIP13 overexpression restored the decrease of c-Myc expression that had been triggered by KIF18B knockdown [45]. These studies suggest that TRIP13

is an upstream regulator of c-Myc and regulates c-Myc expression by stabilizing it. However, some studies suggested that upregulation of TRIP13 was induced by c-MYC-dependent transcriptional activation [46, 47]. To clarify the upstream and downstream relationship between c-Myc and TRIP13, we conducted the rescue experiments and found that TRIP13 knockdown in OSCC cells could downregulate the expression of c-Myc, while TRIP13 overexpression could partially restore the decreased c-Myc expression after triptonide treatment. Our research supported the hypothesis that TRIP13 is located upstream of c-Myc. We speculate that triptonide has the capacity to both directly inhibit c-Myc expression and further reduce c-Myc levels by interfering with TRIP13 expression to promote c-Myc degradation, thus exerting an anticancer effect. However, it is still possible that there is a positive feedback relationship between c-Myc and TRIP13, and further studies are needed to clarify the issue.

In this study, we found for the first time that triptonide was able to inhibit the oncogene TRIP13, revealing its role as a TRIP13 inhibitor, thereby expanding the understanding of the mechanism by which triptonide exerts its anticancer effects, and further confirming its value as an anticancer drug. Furthermore, we have demonstrated, for the first time in OSCC, the association between TRIP13 and c-Myc, two oncogenes, and found that TRIP13 knockdown could inhibit the expression of c-Myc and thus affect the progression of OSCC. Here, we propose the concept of the TRIP13/c-Myc axis, and we suggest that TRIP13 can be used as a target to indirectly inhibit c-Myc expression, as shown by triptonide as a TRIP13 inhibitor to inhibit c-Myc expression. The study provides a new idea for indirectly targeting c-Myc to treat cancer. However, the specific mechanism of interaction between TRIP13 and c-Myc is unclear and needs to be explored by further studies, which is a valuable direction for future research.

There are several limitations of our study that need to be mention. Firstly, only the CLA27 cell line was used for the experiments, which weakens the generalizability of the conclusion. Secondly, the role of TRIP13 in OSCC has not been validated by *in vivo* experiments. Additionally, the effects of triptonide treatment and TRIP13 knockdown on OSCC progression lacked evidence from molecular biology. Finally, this study did not involve specific molecular interaction mechanism, which should be intensively investigated in future studies.

In summary, this study was the first to explore the effect and mechanism of triptonide on OSCC, and demonstrated that triptonide inhibited the progression of OSCC and the expression of c-Myc,

indicating the potential of triptonide as a c-Myc-targeted drug for the treatment of OSCC. Furthermore, our research identified TRIP13 as a target of triptonide, and we investigated its role in OSCC progression, determining that TRIP13 knockdown inhibited OSCC progression. Finally, through rescue experiments, we demonstrated that triptonide reduced c-Myc expression by suppressing TRIP13, thereby inhibiting OSCC progression. The intricate mechanisms through which triptonide exerts its anticancer effects and inhibits c-Myc expression remain to be fully elucidated. Further research is necessary to achieve a more profound and comprehensive understanding of this phenomenon, with the aim of facilitating the development of effective therapeutic strategies for the treatment of OSCC.

Acknowledgements: We appreciate the support from the Jiangsu Province Traditional Chinese Medicine Technology Development Plan (grant number: MS2021041).

Supplementary data are available in the online version of the paper.

References

[1] LING Z, CHENG B, TAO X. Epithelial-to-mesenchymal transition in oral squamous cell carcinoma: Challenges and opportunities. Int J Cancer 2021; 148: 1548-1561. https://doi.org/10.1002/ijc.33352

[2] SUNG H, FERLAY J, SIEGEL RL, LAVERSANNE M, SOERJOMATARAM I et al. Global Cancer Statistics 2020: GLOBOCAN Estimates of Incidence and Mortality Worldwide for 36 Cancers in 185 Countries. CA Cancer J Clin 2021; 71: 209-249. https://doi.org/10.3322/caac.21660

[3] MEIER JK, SCHUDERER JG, ZEMAN F, KLINGELHÖFFER C, HULLMANN M et al. Health-related quality of life: a retrospective study on local vs. microvascular reconstruction in patients with oral cancer. BMC Oral Health 2019; 19: 62. https://doi.org/10.1186/s12903-019-0760-2

[4] SHENG X, LI X, QIAN Y, WANG S, XIAO C. ETS1 regulates NDRG1 to promote the proliferation, migration, and invasion of OSCC. Oral Dis 2024; 30: 977-990. https://doi.org/10.1111/odi.14527

[5] LEEMANS CR, BRAAKHUIS BJ, BRAKENHOFF RH. The molecular biology of head and neck cancer. Nat Rev Cancer 2011; 11: 9-22. https://doi.org/10.1038/nrc2982

[6] NOEL P, VON HOFF DD, SALUJA AK, VELAGAPUDI M, BORAZANCI E et al. Triptolide and Its Derivatives as Cancer Therapies. Trends Pharmacol Sci 2019; 40: 327-341. https://doi.org/10.1016/j.tips.2019.03.002

[7] SONG J, HE GN, DAI L. A comprehensive review on celastrol, triptolide and triptonide: Insights on their pharmacological activity, toxicity, combination therapy, new dosage form and novel drug delivery routes. Biomed Pharmacother 2023; 162: 114705. https://doi.org/10.1016/j.biopha.2023.114705

[8] WANG Z, MU Y, YANG H, GAO Y, JIA Y. Inhibitory effect of triptonide on the malignant behaviors of lung cancer cells by down-regulation of SOX2 expression. J Pharmacol Clin Chin Mater Med 2017; 33: 62-65.

[9] XIANG S, ZHAO Z, ZHANG T, ZHANG B, MENG M et al. Triptonide effectively suppresses gastric tumor growth and metastasis through inhibition of the oncogenic Notch1 and NF-κB signaling pathways. Toxicol Appl Pharmacol 2020; 388: 114870. https://doi.org/10.1016/j.taap.2019.114870

[10] ZHANG M, MENG M, LIU Y, QI J, ZHAO Z et al. Triptonide effectively inhibits triple-negative breast cancer metastasis through concurrent degradation of Twist1 and Notch1 oncoproteins. Breast Cancer Res 2021; 23: 116. https://doi.org/10.1186/s13058-021-01488-7

[11] ZHENG L, FANG S, HUI J, RAJAMANICKAM V, CHEN M et al. Triptonide Modulates MAPK Signaling Pathways and Exerts Anticancer Effects via ER Stress-Mediated Apoptosis Induction in Human Osteosarcoma Cells. Cancer Manag Res 2020; 12: 5919-5929. https://doi.org/10.2147/CMAR.S258203

[12] YANG P, DONG F, ZHOU Q. Triptonide acts as a novel potent anti-lymphoma agent with low toxicity mainly through inhibition of proto-oncogene Lyn transcription and suppression of Lyn signal pathway. Toxicol Lett 2017; 278: 9-17. https://doi.org/10.1016/j.toxlet.2017.06.010

[13] LLOMBART V, MANSOUR MR. Therapeutic targeting of "undruggable" MYC. EBioMedicine 2022; 75: 103756. https://doi.org/10.1016/j.ebiom.2021.103756

[14] GAO FY, LI XT, XU K, WANG RT, GUAN XX. c-MYC mediates the crosstalk between breast cancer cells and tumor microenvironment. Cell Commun Signal 2023; 21: 28. https://doi.org/10.1186/s12964-023-01043-1

[15] DHANASEKARAN R, DEUTZMANN A, MAHAUAD-FERNANDEZ WD, HANSEN AS, GOUW AM et al. The MYC oncogene - the grand orchestrator of cancer growth and immune evasion. Nat Rev Clin Oncol 2022; 19: 23-36. https://doi.org/10.1038/s41571-021-00549-2

[16] GABAY M, LI Y, FELSHER DW. MYC activation is a hallmark of cancer initiation and maintenance. Cold Spring Harb Perspect Med 2014; 4: a014241. https://doi.org/10.1101/cshperspect.a014241

[17] DE LIMA MAP, CAVALCANTE RB, DA SILVA CGL, NOGUEIRA RLM, MACEDO GEC et al. Evaluation of HPV and EBV in OSCC and the expression of p53, p16, E-cadherin, COX-2, MYC, and MLH1. Oral Dis 2022; 28: 1104-1122. https://doi.org/10.1111/odi.13814

[18] MARCONI GD, DELLA ROCCA Y, FONTICOLI L, MELFI F, RAJAN TS et al. C-Myc Expression in Oral Squamous Cell Carcinoma: Molecular Mechanisms in Cell Survival and Cancer Progression. Pharmaceuticals (Basel) 2022; 15: 890. https://doi.org/10.3390/ph15070890

[19] ZHAO S, AN L, YANG X, WEI Z, ZHANG H et al. Identification and validation of the role of c-Myc in head and neck squamous cell carcinoma. Front Oncol 2022; 12: 820587. https://doi.org/10.3389/fonc.2022.820587

[20] PAN Y, MENG M, ZHENG N, CAO Z, YANG P et al. Targeting of multiple senescence-promoting genes and signaling pathways by triptonide induces complete senescence of acute myeloid leukemia cells. Biochem Pharmacol 2017; 126: 34-50. https://doi.org/10.1016/j.bcp.2016.11.024

[21] XU Y, WANG P, LI M, WU Z, LI X et al. Natural small molecule triptonide inhibits lethal acute myeloid leukemia with FLT3-ITD mutation by targeting Hedgehog/FLT3 signaling. Biomed Pharmacother 2021; 133: 111054. https://doi.org/10.1016/j.biopha.2020.111054

[22] AGARWAL S, AFAQ F, BAJPAI P, KIM HG, ELKHOLY A et al. DCZ0415, a small-molecule inhibitor targeting TRIP13, inhibits EMT and metastasis via inactivation of the FGFR4/STAT3 axis and the Wnt/β-catenin pathway in colorectal cancer. Mol Oncol 2022; 16: 1728-1745. https://doi.org/10.1002/1878-0261.13201

[23] LIU X, SHEN X, ZHANG J. TRIP13 exerts a cancer-promoting role in cervical cancer by enhancing Wnt/β-catenin signaling via ACTN4. Environ Toxicol 2021; 36: 1829-1840. https://doi.org/10.1002/tox.23303

[24] YU L, XIAO Y, ZHOU X, WANG J, CHEN S et al. TRIP13 interference inhibits the proliferation and metastasis of thyroid cancer cells through regulating TTC5/p53 pathway and epithelial-mesenchymal transition related genes expression. Biomed Pharmacother 2019; 120: 109508. https://doi.org/10.1016/j.biopha.2019.109508

[25] SHENG N, YAN L, WU K, YOU W, GONG J et al. TRIP13 promotes tumor growth and is associated with poor prognosis in colorectal cancer. Cell Death Dis 2018; 9: 402. https://doi.org/10.1038/s41419-018-0434-z

[26] GAO Y, LIU S, GUO Q, ZHANG S, ZHAO Y et al. Increased expression of TRIP13 drives the tumorigenesis of bladder cancer in association with the EGFR signaling pathway. Int J Biol Sci 2019; 15:1488-1499. https://doi.org/10.7150/ijbs.32718

[27] BANERJEE R, RUSSO N, LIU M, BASRUR V, BELLILE E et al. TRIP13 promotes error-prone nonhomologous end joining and induces chemoresistance in head and neck cancer. Nat Commun 2014; 5: 4527. https://doi.org/10.1038/ncomms5527 Erratum in: Nat Commun 2016; 24;7: 10726. https://doi.org/10.1038/ncomms10726

[28] BANERJEE R, LIU M, BELLILE E, SCHMITD LB, GOTO M et al. Phosphorylation of TRIP13 at Y56 induces radiation resistance but sensitizes head and neck cancer to cetuximab. Mol Ther 2022; 30: 468-484. https://doi.org/10.1016/j.ymthe.2021.06.009

[29] YIN X, HAN S, SONG C, ZOU H, WEI Z et al. Metformin enhances gefitinib efficacy by interfering with interactions between tumor-associated macrophages and head and neck squamous cell carcinoma cells. Cell Oncol (Dordr) 2019; 42: 459-475. https://doi.org/10.1007/s13402-019-00446-y

[30] TANG Z, LI C, KANG B, GAO G, LI C et al. GEPIA: a web server for cancer and normal gene expression profiling and interactive analyses. Nucleic Acids Res 2017; 45: W98-W102. https://doi.org/10.1093/nar/gkx247

[31] HU DD, CHEN XL, XIAO XR, WANG YK, LIU F et al. Comparative metabolism of tripolide and triptonide using metabolomics. Food Chem Toxicol 2018; 115: 98-108. https://doi.org/10.1016/j.fct.2018.03.009

[32] YANG P, DONG F, ZHOU Q. Triptonide acts as a novel potent anti-lymphoma agent with low toxicity mainly through inhibition of proto-oncogene Lyn transcription and suppression of Lyn signal pathway. Toxicol Lett 2017; 278: 9-17. https://doi.org/10.1016/j.toxlet.2017.06.010

[33] LI XX, DU FY, LIU HX, JI JB, XING J. Investigation of the active components in Tripterygium wilfordii leading to its acute hepatotoxicty and nephrotoxicity. J Ethnopharmacol 2015; 162: 238-243. https://doi.org/10.1016/j.jep.2015.01.004

[34] CHANG Z, QIN W, ZHENG H, SCHEGG K, HAN L et al. Triptonide is a reversible non-hormonal male contraceptive agent in mice and non-human primates. Nat Commun 2021; 12: 1253. https://doi.org/10.1038/s41467-021-21517-5

[35] DANG CV, O'DONNELL KA, ZELLER KI, NGUYEN T, OSTHUS RC et al. The c-Myc target gene network. Semin Cancer Biol 2006; 16: 253-264. https://doi.org/10.1016/j.semcancer.2006.07.014

[36] BALUAPURI A, WOLF E, EILERS M. Target gene-independent functions of MYC oncoproteins. Nat Rev Mol Cell Biol 2020; 21: 255-267. https://doi.org/10.1038/s41580-020-0215-2

[37] BERNARD S, EILERS M. Control of cell proliferation and growth by Myc proteins. Results Probl Cell Differ 2006; 42: 329-342. https://doi.org/10.1007/400_004

[38] BRETONES G, DELGADO MD, LEÓN J. Myc and cell cycle control. Biochim Biophys Acta 2015; 1849: 506-516. https://doi.org/10.1016/j.bbagrm.2014.03.013

[39] DOMINGUEZ-SOLA D, YING CY, GRANDORI C, RUGGIERO L, CHEN B et al. Non-transcriptional control of DNA replication by c-Myc. Nature 2007; 448: 445-451. https://doi.org/10.1038/nature05953

[40] WHITFIELD JR, BEAULIEU ME, SOUCEK L. Strategies to Inhibit Myc and Their Clinical Applicability. Front Cell Dev Biol 2017; 5: 10. https://doi.org/10.3389/fcell.2017.00010

[41] LLOMBART V, MANSOUR MR. Therapeutic targeting of "undruggable" MYC. EBioMedicine 2022; 75: 103756. https://doi.org/10.1016/j.ebiom.2021.103756

[42] WANG SS, LV Y, XU XC, ZUO Y, SONG Y et al. Triptonide inhibits human nasopharyngeal carcinoma cell growth via disrupting Lnc-RNA THOR-IGF2BP1 signaling. Cancer Lett 2019; 443: 13-24. https://doi.org/10.1016/j.canlet.2018.11.028

[43] CAI W, NI W, JIN Y, LI Y. TRIP13 promotes lung cancer cell growth and metastasis through AKT/mTORC1/c-Myc signaling. Cancer Biomark 2021; 30: 237-248. https://doi.org/10.3233/CBM-200039

[44] ZHANG G, ZHU Q, FU G, HOU J, HU X et al. TRIP13 promotes the cell proliferation, migration and invasion of glioblastoma through the FBXW7/c-MYC axis. Br J Cancer 2019; 121: 1069-1078. https://doi.org/10.1038/s41416-019-0633-0

[45] LIU L, ZHANG Z, XIA X, LEI J. KIF18B promotes breast cancer cell proliferation, migration and invasion by targeting TRIP13 and activating the Wnt/β-catenin signaling pathway. Oncol Lett 2022; 23: 112. https://doi.org/10.3892/ol.2022.13232

[46] LI Z, LIU J, CHEN T, SUN R, LIU Z et al. HMGA1-TRIP13 axis promotes stemness and epithelial mesenchymal transition of perihilar cholangiocarcinoma in a positive feedback loop dependent on c-Myc. J Exp Clin Cancer Res 2021; 40: 86. https://doi.org/10.1186/s13046-021-01890-1

[47] ZHOU K, ZHANG W, ZHANG Q, GUI R, ZHAO H et al. Loss of thyroid hormone receptor interactor 13 inhibits cell proliferation and survival in human chronic lymphocytic leukemia. Oncotarget 2017; 8: 25469-25481. https://doi.org/10.18632/oncotarget.16038

Figure Legends

Figure 1. Triptonide inhibited the progression of OSCC. A-D) The effects of triptonide on CAL27 cells were detected by CCK-8 assay (A), EdU incorporation assay (B), wound healing assay (C) and transwell assay (D). E) The weights of the NOD-SCID mice and the tumor volumes in the xenograft tumor assay were measured. F) Dissected tumors were weighed and compared. #$p > 0.05$; *$p < 0.05$; **$p < 0.01$; ***$p < 0.001$

Figure 2. Triptonide inhibited the expression of c-Myc in OSCC. A, B) The expression of c-Myc in CAL27 cells was detected by qRT-PCR (A) and WB (B). C) c-Myc expression in xenograft tumors was shown by IHC. *** < 0.001

Figure 3. Triptonide drives transcriptome changes in OSCC cells *in vitro*. A) Heatmap and cluster analysis of global differential expression genes in triptonide-treated CAL27 cells. B, C) Volcano plot depicting the differential expression genes in triptonide-treated CAL27 cells. The differentially expressed genes with a fold change > 2.0 and $p < 0.05$ were indicated by red dots, representing upregulated genes, while genes with a fold change < 0.5 and $p < 0.05$ were indicated by blue dots, representing downregulated genes. D, E) Bar chart (D) and bubble chart (E) of GO enrichment analysis of differential expression genes in triptonide (50 nM)-treated CAL27 cells. F) Bubble chart of GO enrichment analysis of downregulated differential expression genes in triptonide (50 nM)-treated CAL27 cells. G, H) Bubble chart of KEGG pathway enrichment analysis of differential expression genes (G) and downregulated differential expression genes (H) in triptonide (50 nM)-treated CAL27 cells.

Figure 4. TRIP3 was selected as the key differential gene after triptonide treatment. A) Venn diagrams for the number of prominently downregulated genes shared by the differential expression genes in triptonide (50 nM)- and triptonide (100 nM)-treated CAL27 cells. B) TRIP13 mRNA expression profile across all tumor samples and paired normal tissues. C) TRIP13 mRNA expression between HNSCC and paired normal tissues. D) Correlation between MYC and TRIP13 expression in HNSCC. E, F) The expression of TRIP13 in CAL27 cells was detected by qRT-PCR (E) and WB (F). *$p < 0.05$; ***$p < 0.001$

606

607 **Figure 5.** Knockdown of TRIP13 inhibited the progression of OSCC. A, B) The TRIP13
608 knockdown efficiency was verified by qRT-PCR (A) and WB (B). C, D) The effects of TRIP13
609 knockdown on CAL27 cells were detected by CCK-8 assay (A), EdU incorporation assay (B),
610 wound healing assay (C) and transwell assay (D). #p > 0.05; *p < 0.05; **p < 0.01; ***p < 0.001

611

612 **Figure 6.** TRIP13 overexpression partially restored the decreased c-Myc expression after triptonide
613 treatment in OSCC cells. A, B) The TRIP13 overexpression efficiency was verified by qRT-PCR (A)
614 and WB (B). C, D) The expression of c-Myc in CAL27 cells was detected by qRT-PCR (C) and WB
615 (D). #p > 0.05; *p < 0.05; **p < 0.01; ***p < 0.001

Fig. 1 [Download full resolution image]

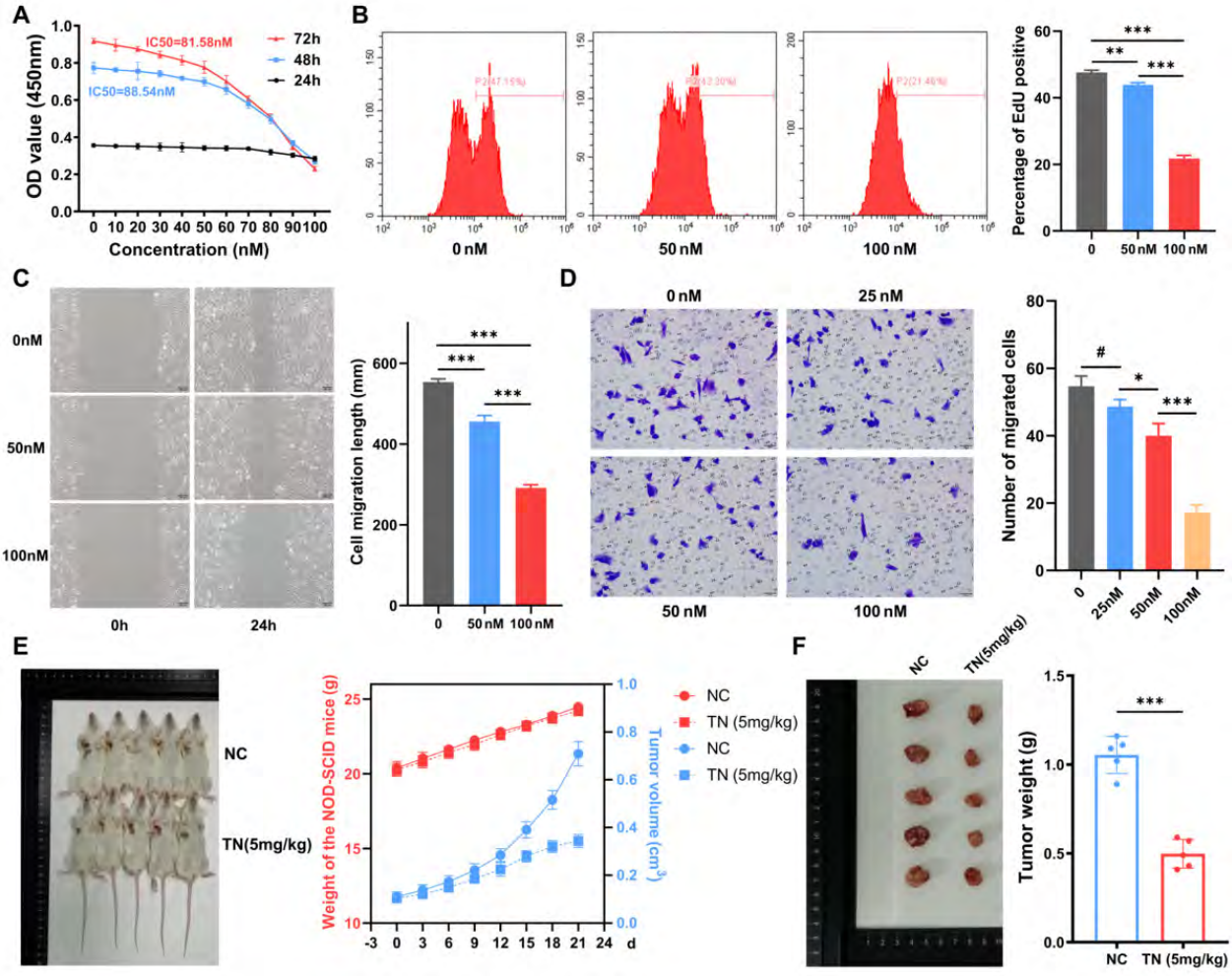

Fig. 2 Download full resolution image

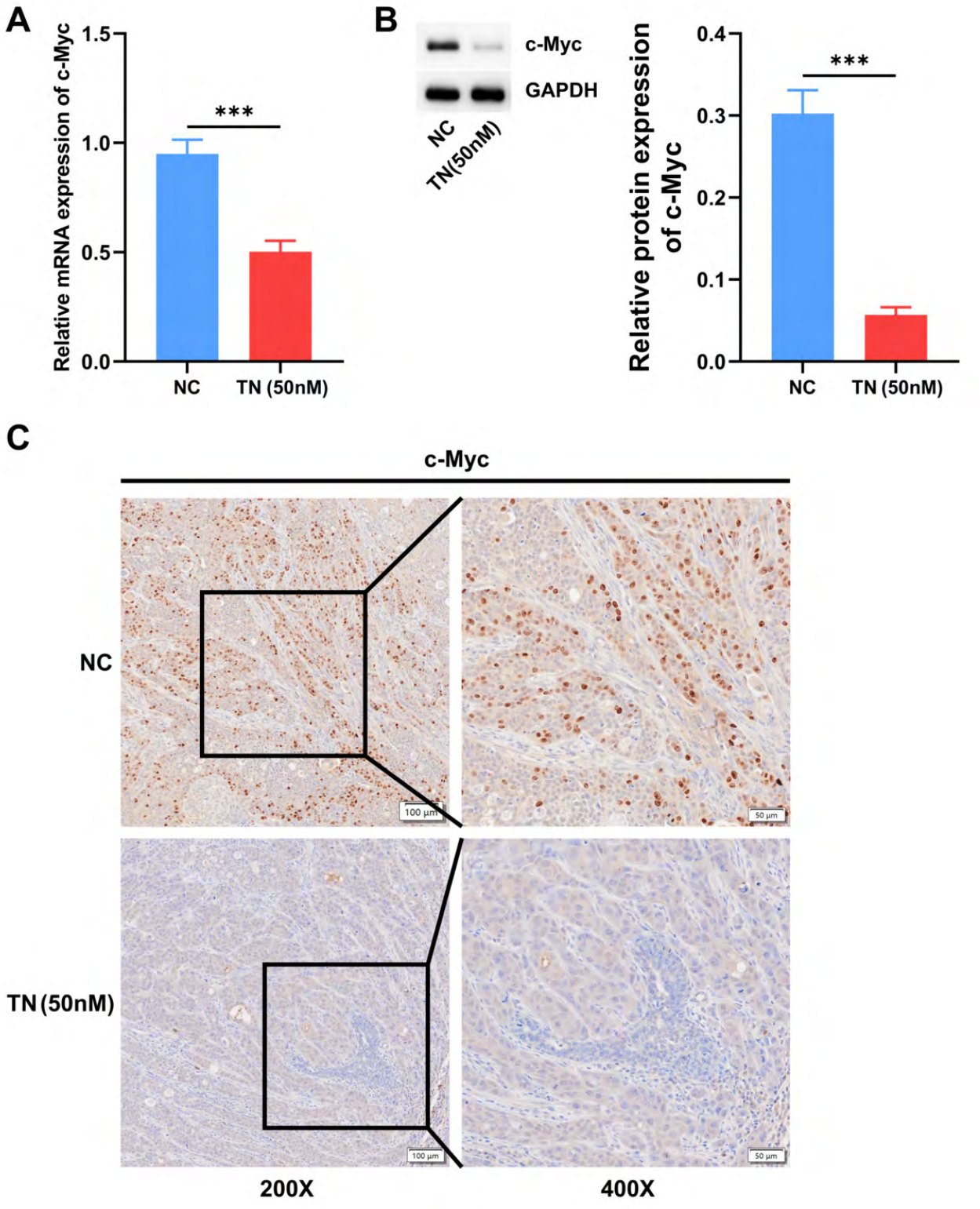

Fig. 3 Download full resolution image

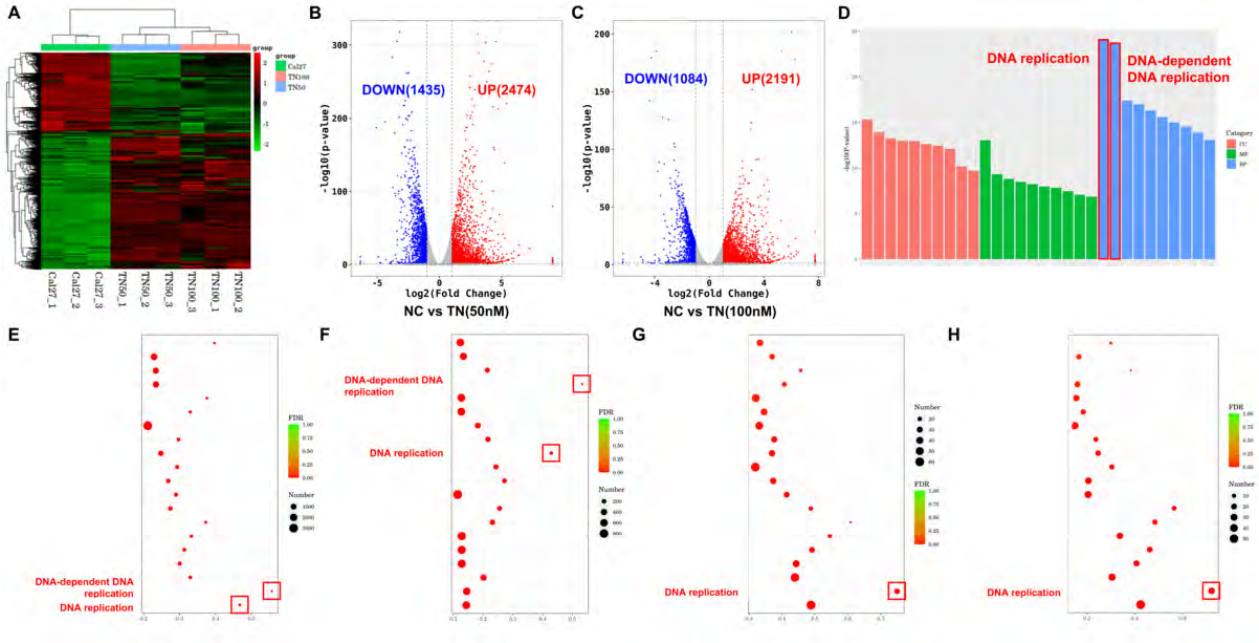

Fig. 4 Download full resolution image

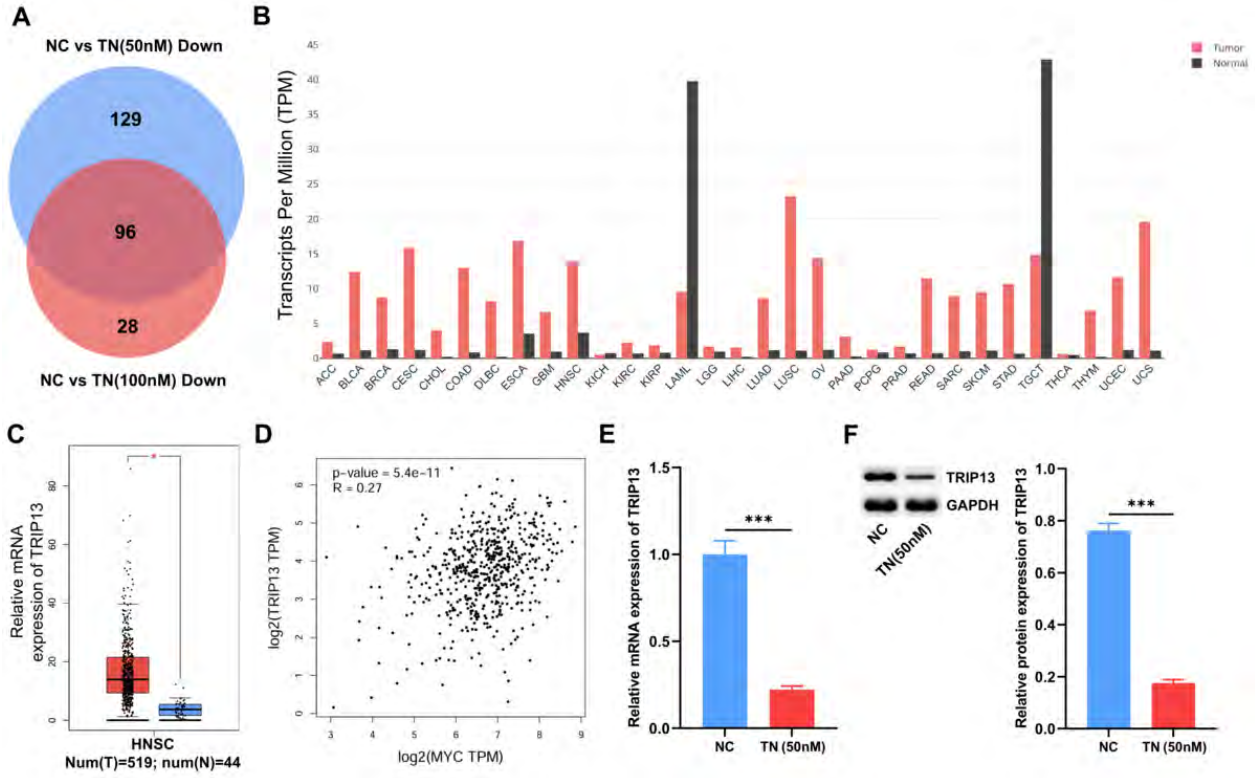

Fig. 5 Download full resolution image

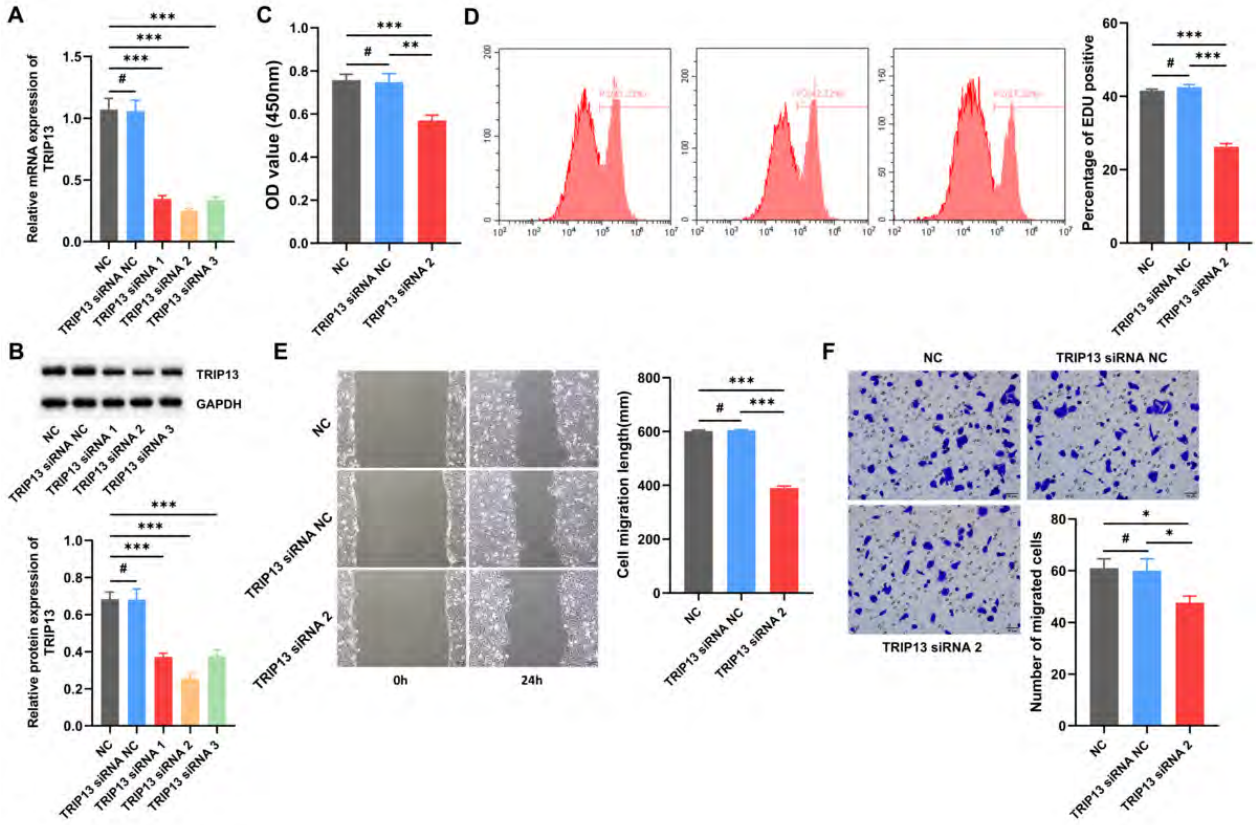

Fig. 6 Download full resolution image